ABCG2, CD44 and SOX9 are increased with the acquisition of drug resistance and involved in cancer stem cell activities in head and neck squamous cell carcinoma cells

KOICHI MURAKAMI[1*], NAOKI UMEMURA[2*], MAKOTO ADACHI[3], MASAHIRO MOTOKI[1] and EMIKA OHKOSHI[1]

[1]Department of Natural Products Chemistry, Faculty of Pharmaceutical Sciences Aomori University, Aomori, Aomori 030-0943; [2]Department of Oral Biochemistry, Asahi University School of Dentistry, Mizuho, Gifu 501-0296; [3]Department of Oral and Maxillofacial Surgery, Nagoya Tokushukai General Hospital, Kasugai, Aichi 487-0016, Japan

Received June 30, 2022; Accepted October 6, 2022

DOI: 10.3892/etm.2022.11658

Abstract. Cancer stem cells are a sub-population of cancer cells with self-renewal activity that play key roles in tumor resistance to chemotherapy and radiation. Several cancer stem cell markers have been identified to correlate with clinical prognosis. However, which marker is associated with which cancer stem cell characteristic is unclear. The present study aimed to clarify the relationship between cancer stem cell markers associated with drug resistance acquisition and the characteristics of cancer stem cells. We generated cisplatin-resistant head and neck squamous cell carcinoma cells by culturing cells in increasing concentrations of cisplatin. The cisplatin-resistant head and neck squamous cell carcinoma cells also acquired multidrug resistance and were named resistant HSC-3 (R HSC-3) cells. R HSC-3 showed no differences in cell proliferation or cell cycle distributions compared with parental cells. R HSC-3 cells showed increased drug excretion ability and elevated expression of ATP-binding cassette subfamily G member 2 (ABCG2), a drug excretion pump. R HSC-3 cells also highly expressed CD44, a cancer stem cell marker, and exhibited enhanced cell invasion and spheroid formation abilities. Furthermore, the stem cell-related factor SRY-box transcription factor 9 (SOX9) was identified as increased in R HSC-3 cells by microarray analysis. Knockdown experiments showed that SOX9 and ABCG2 were involved in the drug excretion ability of R HSC3 cells and ABCG2 was involved in the spheroid formation ability of R HSC-3 cells. These results indicate that CD44, SOX9 and ABCG2 expression levels were enhanced in head and neck squamous cell carcinoma cells that acquired multidrug resistance and that these molecules are important for maintaining cancer stem cell characteristics. Overall, regulating CD44, SOX9 and ABCG2 may be a strategy to inhibit cancer stem cells.

Correspondence to: Dr Naoki Umemura, Department of Oral Biochemistry, Asahi University School of Dentistry, 1851 Hozumi, Mizuho, Gifu 501-0296, Japan
E-mail: umemura@dent.asahi-u.ac.jp

*Contributed equally

Abbreviations: ABCG2, ATP-binding cassette subfamily G member 2; DMEM, Dulbecco's modified Eagle's medium; siRNA, small interfering RNA

Key words: ABCG2, CD44 antigen, cisplatin resistance, chemotherapeutic drug, head and neck squamous cell carcinoma, SRY-box transcription factor 9

Introduction

Cancer stem cells (CSCs) are a minor population of cells within tumors that show high self-renewal ability and have the capacity for differentiation, resulting in cancer cell heterogeneity and thus playing a key role in tumor development (1). In a minimum definition, CSCs exhibit stem cell-like self-renewal properties and high differentiation ability (2,3). Previous studies have shown that CSCs or cancer initiating cells are significantly correlated with poor prognosis (4,5) and resistance to tumor treatments including radiation and chemotherapy (6,7). CSCs represent a small population that are in a quiescent state; thus, they show resistance to some chemotherapies that target the cell cycle and remain in tumors after treatment. CSCs are thus considered to be the cells that initiate recurrence (8). Research has focused on CSC markers as novel targets for cancer treatment.

Various molecules associated with clinical prognosis or recurrence have been reported as CSC markers. CD44 has been well established as a CSC marker in numerous tumor types (9). In our previous study, we showed that induction of CD44, a CSC marker in head and neck squamous cell carcinoma, caused resistance to apoptosis in response to DNA damage (10). We also showed that combination chemotherapy inhibited tumor recurrence in a head and neck squamous cell carcinoma xenograft mouse model, possibly through suppressing the expression of CD44 (11).

Several studies have explored the mechanism of drug resistance acquisition in tumors. Some reports indicated

that drug resistance is acquired after expression of drug excretion pumps, including multidrug resistance mutation 1 (MDR1) and ATP-binding cassette subfamily G member 2 (ABCG2) (12,13). ABCG2 is significantly expressed and drug resistant inside population cells, which exhibit characteristics of CSCs of head and neck squamous cell carcinoma (14,15). Clinically, ABCG2 positivity is significantly correlated with poor prognosis in right-sided colon cancer (16). CSCs have been demonstrated to express drug efflux transporters. Notably, MDR1 and ABCG2 are also CSC markers in several types of tumors including head and neck cancer (16,17).

Various CSC markers related to clinical prognosis have been reported. However, the association between these CSC markers and the characteristics of CSCs at the cellular level is unknown. Whether the developed cancer cells that acquire multidrug-resistance express CSC markers is unknown, and whether the markers are associated with CSC characteristics is unclear.

Cisplatin is used as the first-line chemotherapy treatment of head and neck squamous cell carcinoma in clinical practice (18). In this study, we investigated how CSC markers are related to the characteristics of CSCs such as self-renewal ability, pluripotency, drug resistance, and cell invasion ability in cisplatin-resistant HNSCC cells.

Materials and methods

Cell culture and generation of cisplatin-resistant cells. The HNSCC cell line HSC-3 was obtained from Riken Cell Bank (Ibaraki, Japan). Cells were cultured in Dulbecco's modified Eagle's medium (DMEM; Life Technologies Japan Ltd., Yokohama, Japan) supplemented with 10% fetal bovine serum (FBS; Life Technologies Japan Ltd.) and antibiotics (100 U/ml penicillin and 100 μg/ml streptomycin 25 μg/ml) at 37˚C in a humidified atmosphere containing 5% CO_2.

To generate cisplatin-resistant cells, HSC-3 cells were initially cultured in medium containing 1 μM cisplatin; the cisplatin concentration was then slowly increased up to 100 μM. The generated cell line was viable in medium containing cisplatin at 200 μM for over 2 days.

Cell viability assay. The viability of cells treated with various drugs was measured using 3-(4,5-dimethylthiazol-2-yl)-2,5-diphenyltetrazolium bromide with a Cell Proliferation Kit I (Roche Diagnostics, Mannheim, Germany) following the manufacturer's instructions. The absorbance was measured at 595 nm with a TECAN SpectraFluor plus XFluor4 software (Tecan Japan Co., Ltd.). All data are presented as the means ± standard deviations of at least three independent experiments. To calculate the half maximal inhibitory concentration (IC_{50}), a cell proliferation curve was created from the cell viability assay; the value that inhibited cell proliferation by 50% was calculated. The IC_{50} value was determined from the results from at least three experiments.

Immunofluorescence. Cells were cultured for 48 h in six-well covered glass chamber slides. After two washes with phosphate-buffered saline (PBS) containing 1% bovine serum albumin (Sigma-Aldrich), cell surface Fc receptors were blocked with IgG (Santa Cruz Biotechnology Inc.) on ice for 15 min. The cells were then stained with a 1:100 dilution of a fluorescein isothiocyanate (FITC)-conjugated anti-CD44 monoclonal antibody (BD Biosciences) or an isotype-matched FITC-conjugated IgG control antibody (BD Biosciences) for 30 min at 37˚C. After washing, the cells were analyzed using an ECLIPSE Ti-U microscope equipped with an Intensilight C-HGFI illumination system (Nikon Co., Ltd.). Digital images were processed with NIS Elements D version 4.0 imaging software (Nikon Co., Ltd.) and Adobe Photoshop elements 10 version 10.0 (Adobe Systems).

Efflux pump assay. Cells ($1x10^5$ cells) were plated in 96-well tissue culture plates, wall black/clear bottom (Sigma-Aldrich) and cultured overnight. After cells achieved 70% confluency, the medium was aspirated and cells were washed twice with PBS(+) with glucose buffer: PBS with $CaCl_2 \cdot 2H_2O$ (0.9 mM), $MgCl_2 \cdot 12H_20$ (0.33 mM) and glucose (10 mM). Next, 100 μl PBS(+) with glucose buffer was added per well and cells were incubated for 1 h at 37˚C. The buffer was aspirated and replaced with 100 μl Calcein-AM (4 mM solution; PromoKine, Heidelberg, Germany) in DMEM and the plate was incubated for 1 h at 37˚C. After aspiration of the medium, cells were washed with ice-cold PBS(+) and lysed in 100 μl 1% SDS/PBS for 10 min in the dark at room temperature. Calcein incorporated into cells, indicated by intense yellow-green fluorescence, was assessed using TECAN SpectraFluor plus XFluor4 software (Tecan Japan Co., Ltd., Kawasaki, Japan). All data are presented as the means ± standard deviations of at least three independent experiments.

Immunoblot analysis. Whole-cell extracts were obtained with a lysis buffer (10x Cell Lysis buffer; Cell Signaling Technology, Beverly, MA, USA) supplemented with 1 mM PMSF and one tablet of protease inhibitor cocktail (Complete, EDTA-free; Roche Diagnostics GmbH). Protein concentrations were assayed, and equal amounts of protein were subjected to 8% SDS-polyacrylamide gel electrophoresis, followed by immunoblotting with anti-CD44 mouse monoclonal antibody, anti-cleaved PARP rabbit monoclonal antibody, anti-SOX9 rabbit monoclonal antibody, anti-E-cadherin mouse monoclonal antibody, anti-Vimentin rabbit monoclonal antibody, anti-FGF9 rabbit monoclonal antibody (all from Cell Signaling Technology), anti-breast cancer resistance protein (ABCG2) rabbit polyclonal antibody and anti-β-actin antibody (Sigma-Aldrich). Membranes were then incubated with corresponding peroxidase-conjugated secondary antibodies (anti-rabbit IgG antibody or anti-mouse IgG antibody; Cell Signaling Technology), and the positive bands were visualized by chemoluminescence (Clarity™ Western ECL substrate; Bio-Rad). The images were developed with an ImageQuant™ LAS500 Imaging System (GE Healthcare Bio-Sciences AB). For semi-quantitative analysis of protein expression, the protein bands were quantified by densitometry using Image J (National Institutes of Health). The expression of the target protein relative to the expression of β-actin was calculated.

Flow cytometry analysis. Cells were harvested by trypsinization, washed with PBS (-), and centrifuged; cell pellets were resuspended in FACS buffer (PBS containing 0.5% bovine serum albumin). The cells were stained for 30 min at 4˚C with a

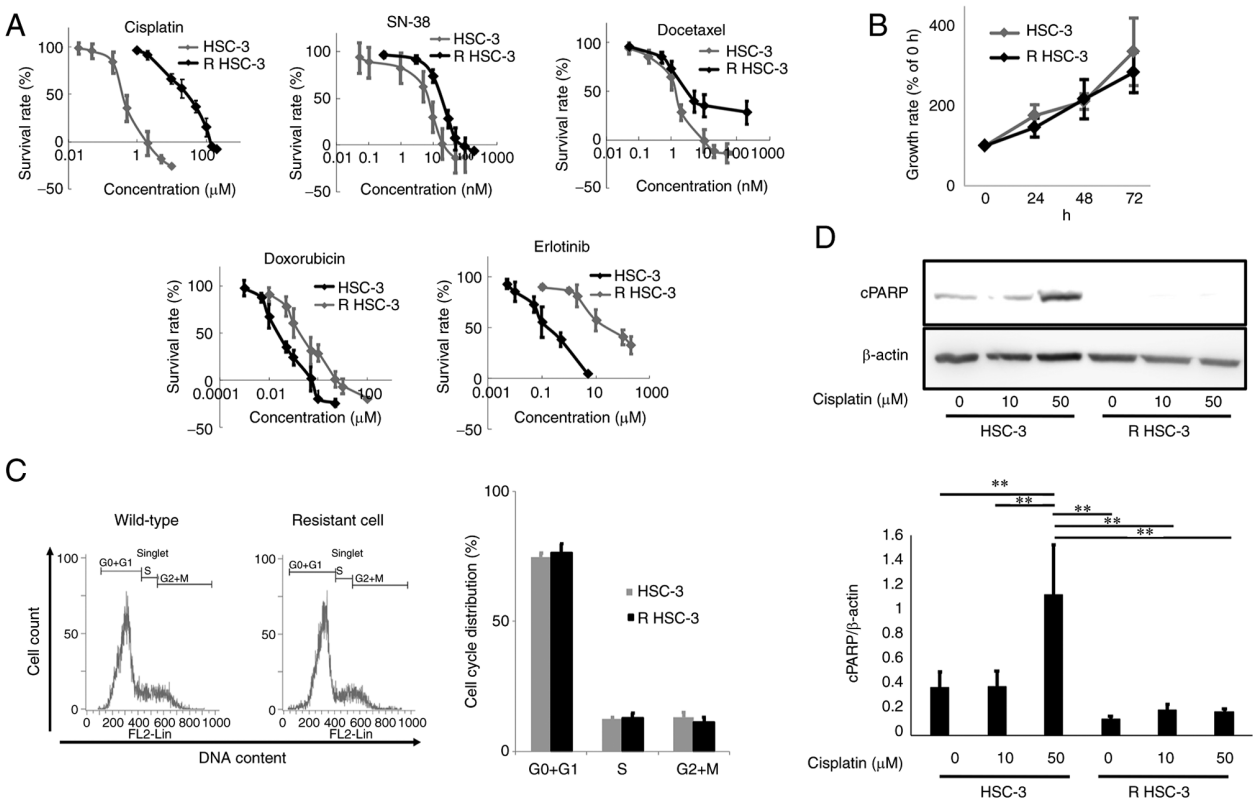

Figure 1. Cisplatin-resistant head and neck squamous cell carcinoma cells acquire multidrug resistance. (A) Cell proliferation curves of the parental HSC-3 and R HSC-3 cell lines treated with cisplatin, SN-38, docetaxel, doxorubicin and erlotinib are presented. Data at each time point was determined by setting the initial number at seeding as 100%. Data are presented as the mean ± standard deviation (n=3). (B) Cell proliferation rate of HSC-3and R HSC-3 cells. Student's t-test HSC-3 vs R HSC-3. (C) Representative histograms of cell cycle analysis and % of cells in each cell cycle phase. (D) Western blotting of the apoptosis marker cleaved PARP in cells treated with cisplatin for 24 h. **P<0.01. R HSC-3, drug-resistant HSC-3; PARP, poly (ADP-ribose) polymerase; cPARP, cleaved PARP.

FITC-conjugated anti-human CD44 antibody (BD Biosciences, San Jose, CA, USA) or an isotype-matched FITC-conjugated IgG control antibody (BD Biosciences). Data acquisition and analysis were performed using an EC800 Flow Cytometry Analyzer with EC800 analysis software (Sony Biotechnology Inc.). All data are presented as the means ± standard deviations of at least three independent experiments.

Real-time polymerase chain reaction. Total RNA was purified using the RNeasy Mini kit (Qiagen), and 600 ng of total RNA was used for reverse transcription with an iScript™ Advanced cDNA Synthesis Kit (Bio-Rad). The real-time polymerase chain reaction contained 1 μl of cDNA sample diluted 20x, 1 μl each of forward and reverse primers (final, 500 nM), 7 μl of nuclease-free water, and 10 μl of SsoAdvanced SYBR Green Supermix (Bio-Rad). The Bio-Rad PrimePCR assay system was used with the following primers: PrimePCR™ SYBR Green Assay: ABCG2, human; or PrimePCR™ SYBR Green Assay: CD44, human. As a control, we used PrimePCR™ SYBR Green Assay: GAPDH, human. The reaction cycles were an initial 5 min at 95˚C, followed by 45 cycles of 95˚C for 10 sec and 72˚C for 10 sec. The reactions and absolute quantification analyses were performed with a Thermal Cycler Dice Real Time System TP800 (Takara Bio).

Small interfering RNA (siRNA) transfection. siRNAs specifically targeting human ABCG2 (siRNAs #1 and #2, IDs s18056 and s18057), CD44 (siRNA #1 and #2, IDs s2681 and s2682), and SOX9 (siRNAs #1 and #2, IDs s13306 and s532658) were obtained from Life Technologies (Carlsbad, CA, USA). Cells were plated in six-well plates ($1x10^5$ per well) and transfected with siRNAs for 3 days in antibiotic-free media using siRNA Lipofectamine RNAiMAX and OPTI-MEM I reduced serum medium (Invitrogen, Carlsbad, CA, USA), in accordance with the Lipofectamine protocol. After 72 h of transfection, the cells were used for experiments. siRNA transfection was confirmed by immuno blotting (Fig. S1). The efficacy of knockdown by siRNAs was determined by calculating the inhibition of protein expression with the following results: siSOX9#1 90.1%, siSOX9#2 93%, siABCG2#1 12%, siABCG2#2 61%, siCD44#1 81%, and siCD44#2 83% (Fig. S1).

Microarray analysis. Total RNA was isolated from HSC-3 and R HSC-3 cell lines using the RNeasy Mini kit (Qiagen) following the manufacturer's instruction. The cRNA was amplified, labeled using an Agilent low-Input QuickAmp labeling Kit, One-color (Agilent Technologies) and then hybridized to a 60K Agilent 60-mer oligomicroarray (SurePrint G3 Human GE microarray 8X60K Ver3.0; Agilent Technologies) following the manufacturer's instructions. The hybridized microarray slides were scanned using an Agilent scanner. Relative hybridization intensities and background hybridization values were calculated using Agilent Feature Extraction Software (9.5.1.1). The raw signal intensities

and flags for each probe were calculated from hybridization intensities (gProcessedSignal) and spot information (gIsSaturated) following the procedures recommended by Agilent (Flag criteria on GeneSpring Software; absent (A): 'Feature is not positive and significant' and 'Feature is not above background', marginal (M): 'Feature is not Uniform', 'Feature is Saturated', and 'Feature is a population outlier', and Present (P): others). The raw signal intensities of all samples were normalized by quantile algorithm with 'preprocessCore' library package (19) on Bioconductor software (20). To identify up- and down-regulated genes, we calculated Z-scores (21) and ratios (non-log scaled fold-change) from the normalized signal intensities of each probe for comparison between control and experiment samples. We established the following criteria to identify up- and down-regulated genes: up-regulated genes, Z-score ≥2.0 and ratio ≥1.5-fold; and down-regulated genes, Z-score ≤-2.0 and ratio ≤0.66.

Cell invasion assay. Cell invasion analysis was performed using BD Falcon culture inserts (Becton Dickinson and Company, Franklin Lakes, NJ, USA), which contain 8-μm pores in polyethylene terephthalate membranes. Briefly, $1x10^5$ cells were resuspended in serum-free medium and added to the upper Transwell chamber in a 12-well plate. The lower chamber was filled with serum-free DMEM or DMEM containing 10% fetal bovine serum. After 24 h, cells remaining on the upper surface of the membrane were removed with a cell scraper. Invaded cells to the membrane were fixed with cold 6.0% (v/v) glutaraldehyde for 30 min and stained with 0.5% (w/v) crystal violet. Cells were counted in 10 high-power microscope fields. All data are presented as the means ± standard deviations of at least three independent experiments.

Statistical analysis. All quantitative data are presented as the mean ± SD. Data from multiple groups were evaluated using one-way analysis of variance followed by Tukey-Kramer test in Fig. 1D, 3A, 3B and 4B. A paired student's T test was performed to compare two groups in Fig. 1B, 1C, 2A, 2B and 2D. Values of $P<0.05$ were considered statistically significant. All statistical analyses were performed using Statistics Analysis software for Mac Ver. 3.0 (Esumi Co. Ltd., Tokyo, Japan).

Results

Cisplatin-resistant head and neck squamous cell carcinoma cells acquire multidrug resistance. In this study, we used the human head and neck squamous cell carcinoma cell line HSC-3. To establish cisplatin-resistant cells, we cultured cells in the presence of a low concentration (1 μM) of cisplatin and continued the cell culture with gradually increasing concentrations of cisplatin. Finally, we acquired a cell group that maintained survival even with cisplatin 100 μM. The half maximal inhibitory concentration (IC50) of cisplatin in the parental HSC-3 cells was 0.7±0.2 μM, whereas the IC50 of cisplatin-resistant HSC-3 cells was 20.3±6.3 μM (Fig. 1A and Table I). Furthermore, the cisplatin-resistant HSC-3 cells were also resistant to other drugs with different mechanisms of action (Table I). Therefore, we named this multidrug-resistant cell line as resistant HSC-3 cells (R HSC-3).

Table I. Half maximal inhibitory concentration (IC50) of chemotherapy reagents in HSC-3 and R HSC-3 cells.

Treatment	Unit	IC50	HSC-3 R HSC-3
Cisplatin	mM	0.7±0.2	20.3±6.3
SN-38	nM	7.1±1.7	22.2±3.7
Docetaxel	nM	0.9±0.2	6.6±1.2
Erlotinib	mM	0.2±0.04	31.9±2.0
Doxorubicin	nM	26±6	223±16

We evaluated the cell proliferation rate of R HSC-3 cells and found no significant difference in cell proliferation compared with HSC-3 cells (Fig. 1B). Most anti-cancer agents that target the cell cycle exert their effects in cancer cells with abnormal proliferation; these agents do not work for CSCs. CSCs remain in G0 phase (quiescent phase) (22,23) and therefore targeting the quiescent CSCs remains challenging (24).

We also performed cell cycle analysis and found no significant difference in the cell cycle distribution of the drug-resistant and parental cells (Fig. 1C). Notably, R HSC-3 cells treated with cisplatin showed reduced expression of cleaved PARP, which is a marker of apoptosis, compared with the parental HSC-3 cells (Fig. 1D). These data indicated that the R HSC-3 cells showed no significant difference in cell proliferation and cell cycle distribution compared with the parental strain but failed to undergo apoptosis in response to cisplatin.

Increased drug excretion in the multidrug-resistant head and neck squamous cell carcinoma cell line. The expression of drug transporters is closely associated with drug resistance of cancer cells (25), and previous studies indicated that one of the mechanisms for acquiring drug resistance in cancer cells is the aberrant activity of drug efflux pumps in cancer cells (26). Therefore, we next examined the drug efflux function of R HSC-3 cells using calcein-AM efflux assays. In this assay, cells are cultured with cisplatin in the presence of calcein-AM; the uptake of calcein-AM, monitored by fluorescence imaging, reflects the amount of cisplatin in cells. In R HSC-3 cells cultured with cisplatin concentrations ranging from 50 to 200 μM, the intracellular fluorescence did not increase, indicating that the drug excretion ability of R HSC-3 cells was significantly higher ($P<0.01$) than that of parental cells (Fig. 2B). We also found that the ABCG2 transporter was expressed at higher levels in the resistant cells compared with the parental cells (Fig. 2C-D).

We evaluated the expression of CD44, a marker of cancer stem cells in cancer including head and neck cancer, and found that the mRNA and protein levels of CD44 were increased in R HSC-3 cells compared with levels in parental HSC-3 cells (Fig. 2A). Flow cytometric analysis showed that the number of CD44-positive cells in HSC-3 cells was 98%, but that in R HSC-3 was not significantly different from 100%. However, while the mean fluorescence intensity (MFI) was 63.1 in HSC-3 cells, the MRI in R HSC-3 was significantly increased to 150.8 ($P<0.01$) (Fig. 2C and D).

Together, these results showed that head and neck squamous cell carcinoma cells with acquired multidrug resistance

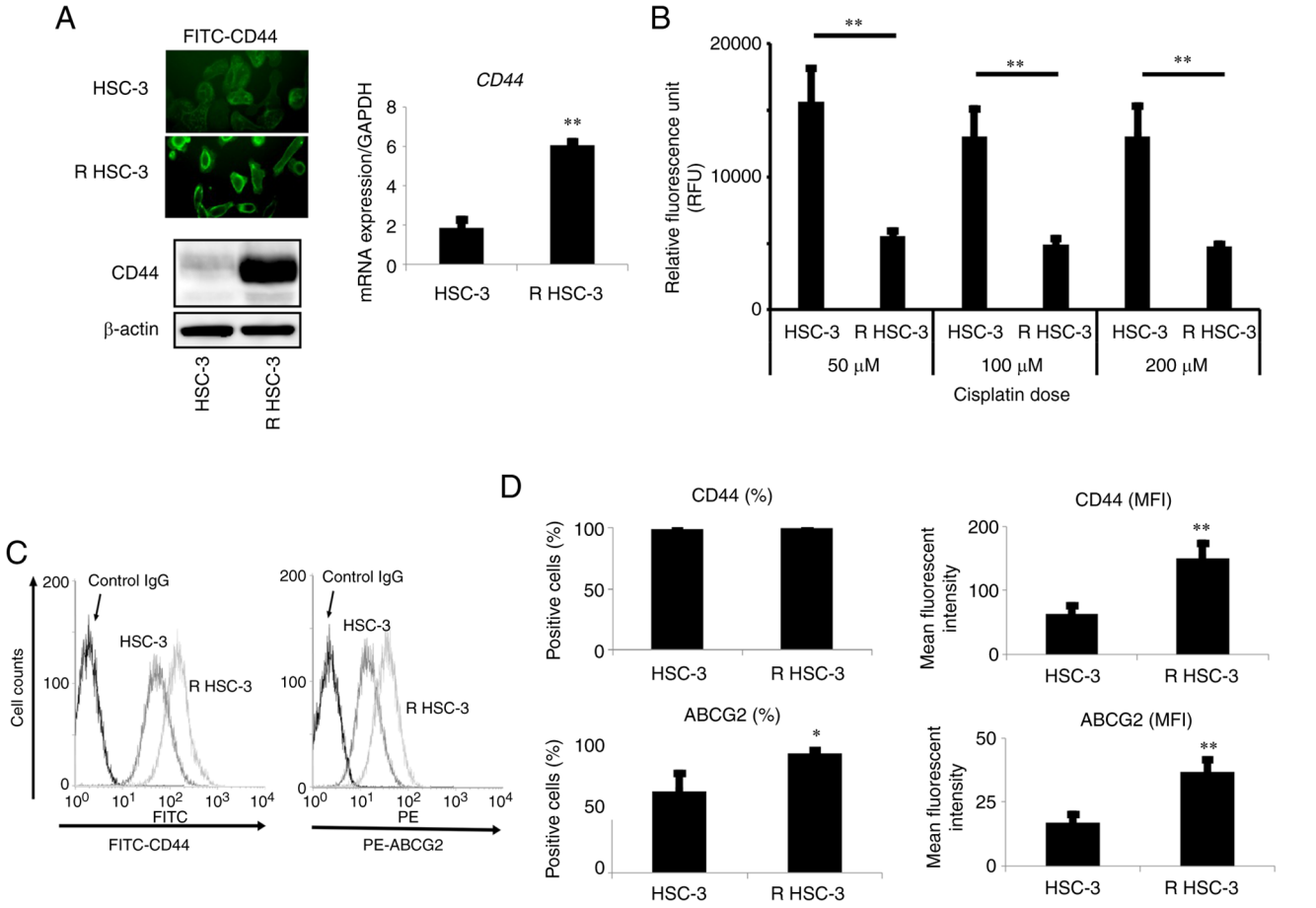

Figure 2. Expression levels of CD44 and ABCG2 are enhanced in acquired multidrug-resistant head and neck squamous cell carcinoma cells. (A) CD44 protein and mRNA expression in HSC-3 and R HSC-3 were determined by immunofluorescence, immunoblotting and reverse transcription-quantitative PCR. (B) Drug efflux pump assay with calcein-AM in cells treated with cisplatin at 50, 100 and 200 μM for 24 h. (C) Flow cytometry evaluation of the expression levels of ABCG2 and CD44. (D) Comparison of % positive cells (left panel) and MFI (right panels) of flow cytometry data. *P<0.05 and **P<0.01 versus HSC-3 cells. ABCG2, ATP-binding cassette subfamily G member 2; R HSC-3, drug-resistant HSC-3; MFI, mean fluorescence intensity.

exhibited increased drug efflux function and elevated expression of the ABCG2 transporter compared with the parental cells. The drug-resistant cells also exhibited increased expression of CD44.

Multidrug-resistant head and neck squamous cell carcinoma cells exhibit characteristics of CSCs. Next, we analyzed the characteristics of R HSC-3 cells. To evaluate the self-renewal ability of cells, we performed spheroid formation assays and found that the formation of spheroids was significantly higher in R HSC-3 cells than in HSC-3 cells (P<0.01) (Fig. 3A). R HSC-3 also showed significantly increased cell invasion (P<0.01) (Fig. 3B). Additionally, R HSC-3 cells showed low E-cadherin and high vimentin expression that characterized an epithelial-mesenchymal transition-phenotype compared with the parental cells (Fig. 3C). These results indicated that the multidrug-resistant head and neck squamous cell carcinoma cells showed enhanced spheroid formation and invasion ability compared with the parental cell line.

Increased expression of SOX9 in multidrug-resistant head and neck squamous cell carcinoma cells. To evaluate the expression of stem cell-related genes in R HSC-3 cells, we performed microarray analysis. We found that the stem cell-related genes *PAX8*, *SOX9*, *NOG*, and *MMP24* were significantly increased and *ETV4*, *METTL3*, *HMGA2*, *SOX2*, and *FGFR3* were significantly decreased (Table II, Fig. 4A). Although we tried to confirm protein level, only SOX9 expression was detected. Immunoblot showed that the expression of SOX9 was significantly increased in R HSC-3 cells compared with parental cells (Fig. 3C). We therefore speculated that SOX9 may also be involved in the characteristics of CSCs in the multidrug-resistant head and neck squamous cell carcinoma cells.

SOX9 has a cell-autonomous effect in Sertoli cells. Furthermore, previous studies revealed that SOX9 upregulates FGF9 to generate a SOX9/fibroblast growth factor 9 (FGF9) feed-forward loop (27). FGF family (including FGF9) signals regulate a variety of cellular processes during embryogenesis and carcinogenesis (28). We found that FGF9 expression was increased in R HSC-3 cells (Fig. 3C).

SOX9, CD44, and ABCG2 are involved in the characteristics of CSCs. We next examined the roles of CD44, SOX9 and ABCG2 in the drug excretion ability, spheroid formation ability, and cell invasion ability of R HSC-3 cells using siRNA-mediated silencing. We found that drug excretion ability was significantly decreased by knockdown of SOX9

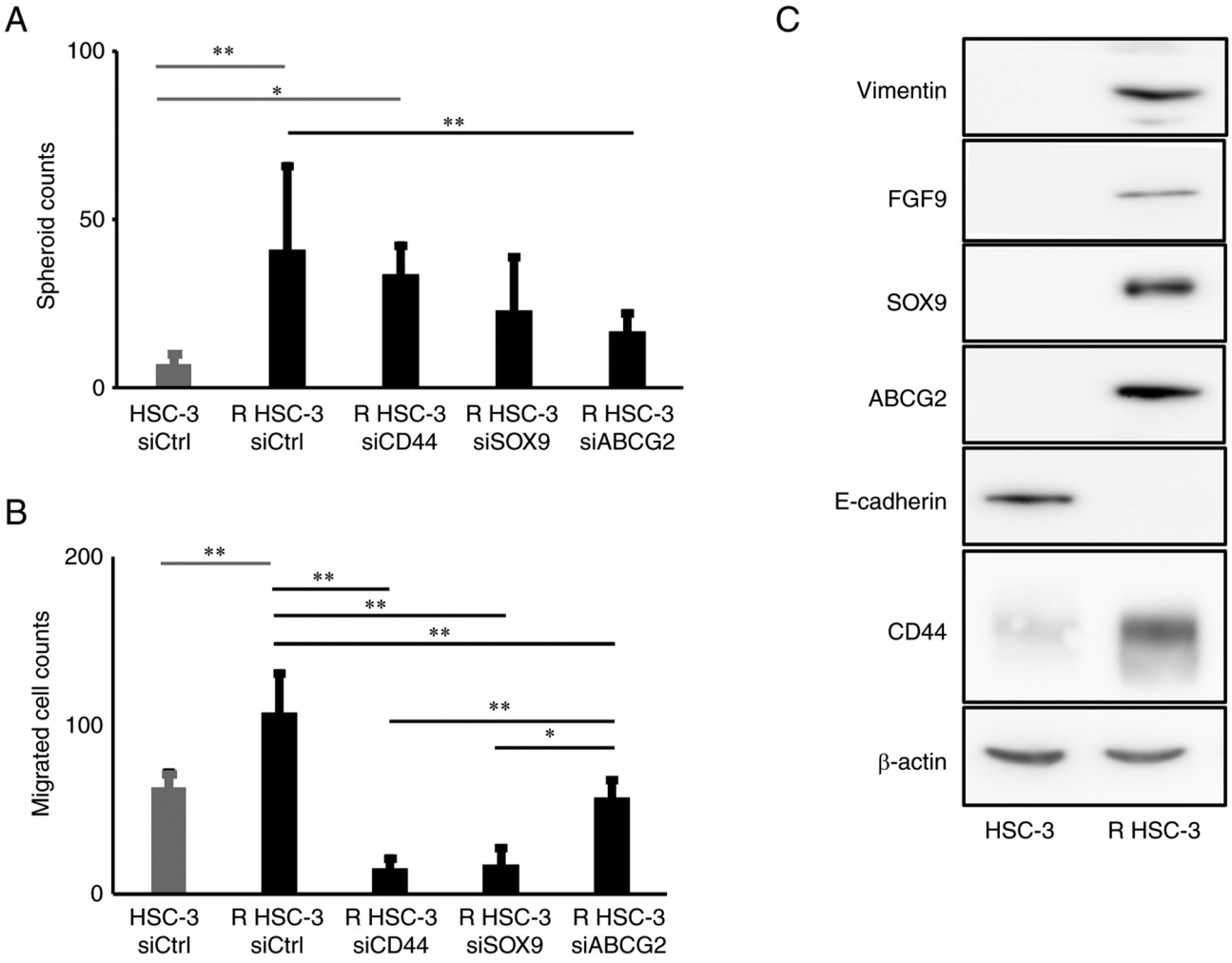

Figure 3. Spheroid formation and invasion ability is increased in acquired multidrug-resistant head and neck squamous cell carcinoma cells. (A) Spheroid-forming ability and (B) cell invasion ability in HSC-3 and R HSC-3 cells with CD44, SOX9 and ABCG2 knockdown. (C) Western blot analysis of cancer stem cell-related molecules and EMT-related proteins in HSC-3 and R HSC-3 cells. *P<0.05 and **P<0.01. ABCG2, ATP-binding cassette subfamily G member 2; R HSC-3, drug-resistant HSC-3; si, short interfering; Ctrl, control; FGF9, Glia-activating factor; SOX9, SRY-box transcription factor 9.

(P<0.05) and by knockdown of ABCG2 (P<0.01) in R HSC-3 cells; in contrast, knockdown of CD44 had no impact on drug excretion activity (Fig. 4B). Furthermore, no significant change was observed in spheroid formation in R HSC-3 cells with knockdown of SOX9 or CD44, but the knockdown of ABCG2 reduced spheroid formation ability (Fig. 3A). We observed a significant decrease (P<0.01) in migration of cells with knockdown of CD44, SOX9, and ABCG2 compared with controls (Fig. 3B).

Discussion

In this study, we generated a drug-resistant head and neck squamous cell carcinoma cell line. We examined whether the multidrug-resistant cells exhibited characteristics of CSCs and which CSC-related molecules are associated with the characteristics of CSCs.

HSC-3 cells were continuously cultured in the presence of cisplatin and acquired resistance to cisplatin. We initially aimed to create cisplatin-resistant head and neck squamous cell lines in several cell lines, including HSC-2, HSC-3, and SAS. However, the cell lines other than HSC-3 gradually died as the concentration of cisplatin increased, and we only obtained cisplatin-resistant HSC-3 cells. The cisplatin-resistant strain also acquired cross-resistance, including resistance to SN-38, docetaxel, doxorubicin, and the molecular-targeted drug erlotinib. The multidrug-resistant cell line did not show any significant changes in cell proliferation compared with the parental cell line. However, the drug excretion ability, cell migration ability, and spheroid-forming ability were enhanced. In addition, the expressions of ABCG2 and CD44 were increased in the drug-resistant cells, and microarray analysis revealed that the expression of SOX9 was also increased. These findings indicated that the multidrug-resistant head and neck squamous cell carcinoma cells exhibited characteristics of cancer stem cells. We further examined the roles of CD44, SOX9, and ABCG2 in the drug excretion ability, cell invasion ability, and spheroid formation ability of multidrug-resistant head and neck squamous carcinoma cells. Our results showed that ABCG2 is involved in spheroid formation, SOX9 and ABCG2 are involved in the drug excretion ability, and CD44, SOX9, and ABCG2 are involved in cell invasion ability of R HSC-3 cells.

CSCs exhibit self-renewal ability and drug tolerance and contribute to tumor metastasis and recurrence (29). However,

Table II. Up- and downregulated stem cell related genes in HSC3 vs. R HSC-3 cells by microarray analysis.

GeneSymbol	Description	Compare1_Zscore	Compare1_ratio
MMP24	Homo sapiens matrix metallopeptidase 24 (membrane-inserted), mRNA [NM_006690]	4.804045	170.8623
NOG	Homo sapiens noggin, mRNA [NM_005450]	4.185133	34.99634
PAX8	Homo sapiens paired box 8, transcript variant PAX8A, mRNA [NM_003466]	2.236811	10.71776
SOX9	Homo sapiens SRY (sex determining region Y)-box 9, mRNA [NM_000346]	2.315078	7.151924
ETV4	Homo sapiens ets variant 4, transcript variant 2, mRNA [NM_001079675]	-2.73807	0.097956
FGFR3	Homo sapiens fibroblast growth factor receptor 3, transcript variant 1, mRNA [NM_000142]	-3.53021	0.110719
HMGA2	Homo sapiens high mobility group AT-hook 2, transcript variant 1, mRNA [NM_003483]	-2.68699	0.207217
METTL3	Homo sapiens methyltransferase like 3, mRNA [NM_019852]	-2.72488	0.147527
SOX2	Homo sapiens SRY (sex-determining region Y)-box 2, mRNA [NM_003106]	-3.90926	0.014163

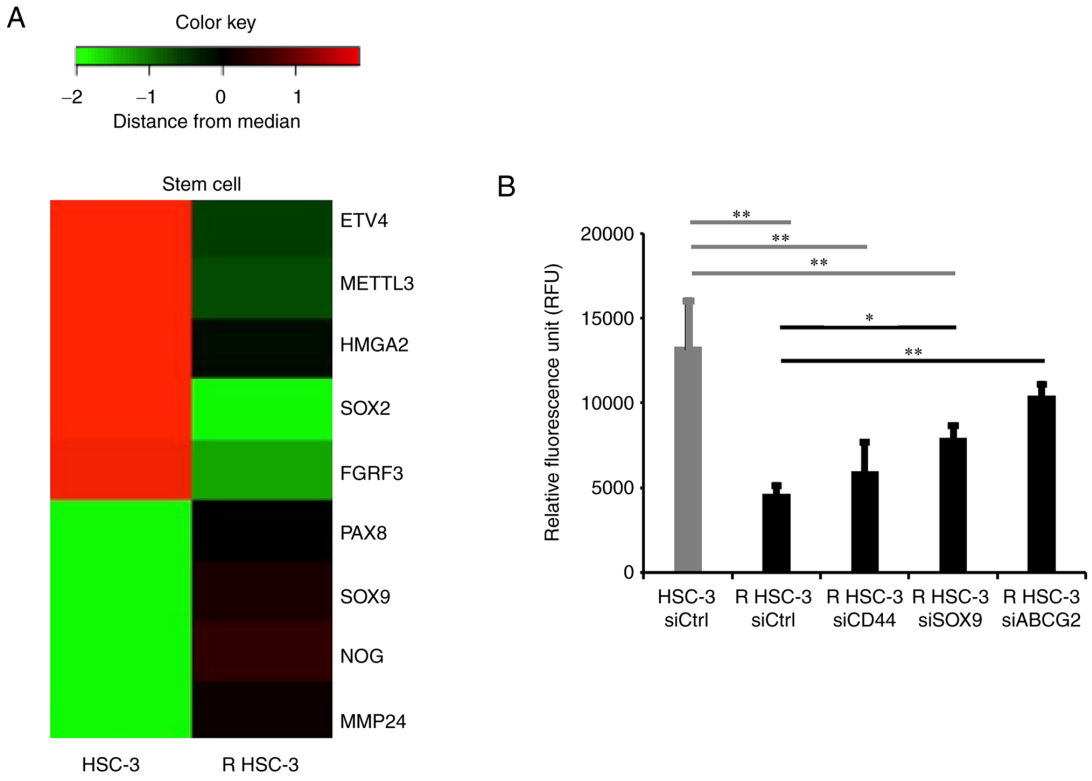

Figure 4. Evaluation of stem cell-related genes by microarray analysis and improvement of drug excretion ability in acquired multidrug-resistant head and neck squamous cell carcinoma cells. (A) Stem cell-related gene expression in HSC-3 and R HSC-3 cells shown on a heat map. (B) Efflux pump assay in cells with CD44, SOX9 and ABCG2 knockdown. *P<0.05 and **P<0.01. R HSC-3, drug-resistant HSC-3; ABCG2, ATP-binding cassette subfamily G member 2; SOX9, SRY-box transcription factor 9; si, short interfering; Ctrl, control; ETV4, ets variant transcription factor 4; METTL3, methyltransferase like 3; HMGA2, high mobility group AT-hook 2; SOX2, SRY-box transcription factor 2; FGFR3, fibroblast growth factor receptor 3; PAX8, paired box 8; NOG, noggin; MMP24, matrix metallopeptidase 24.

the relationship between the acquisition of drug resistance and the expression of CSC markers and the characteristics of CSC such as cell invasion and spheroid formation has not been clarified. In this study, we created a multidrug-resistant head and neck squamous cell carcinoma cell line and analyzed stem cell-related genes by microarray analysis. The results revealed

significantly increased expressions of *PAX8*, *SOX9*, *NOG*, and *MMP24* genes in drug-resistant cells. The molecules were examined by western blotting (data not shown), but only SOX9 was detected. Although this study newly verified the involvement of SOX9 in the characteristics of CSCs, *PAX8*, *NOG*, and *MMP24* will also need further detailed verification in the future. The stem cell-related genes that were significantly reduced by microarray analysis were *ETV4*, *METTL3*, *HMGA2*, *SOX2* and *FGFR3* genes. Future studies should examine why these CSC-related genes tended to decrease with the acquisition of multidrug resistance. In this study, we investigated relationship between expression of CD44, ABCG2, and SOX9 and CSCs properties such as drug excretion ability, cell invasion ability, and spheroid-forming ability. Our results showed that SOX9 and ABCG2 are involved in drug excretion ability, ABCG2 is involved in spheroid formation, and CD44, SOX9, and ABCG2 are involved in cell invasion ability of drug-resistant cells. SOX9 forms a feed-forward loop with FGF9, and we confirmed that FGF9 was also expressed in R HSC-3 cells. These results indicated that SOX9 and FGF9 may operate through a feed-forward loop in head and neck squamous cell carcinoma to promote metastasis and progression.

Early studies showed that the ATP-binding proteins MDR-1 and ABCG2 were involved in drug excretion of cancer cells (30,31). ABCG2-positive cells exhibit drug resistance and epithelial-mesenchymal transition phenotypes (32). Subsequent reports identified ABCG2 as one of the CSC markers for head and neck squamous cell carcinoma (33). In this study, we found that ABCG2, which is involved in drug excretion ability, plays a role in spheroid formation and invasion ability. CD44 is a CSC marker for head and neck squamous cell carcinoma and is significantly associated with prognosis (34,35). Our previous study reported that CD44 is involved in the inhibition of apoptosis induction and induction of CD44 degradation by chemotherapy may be effective in inhibiting tumor recurrence (10,11). We found that CD44 is involved in cell invasion activity of drug-resistant cells. SOX9 is a member of the SRY-related high-mobility group of box transcription factors. Studies showed that SOX9 is mutated in skeletal malformations, XY transsexuals, and campomelic dysplasia characterized by neonatal lethality (36), and SOX9 is important for the differentiation of embryonic stem cells into salivary glands (37). Furthermore, SOX9 is associated with prognosis in lung cancer and breast cancer and a risk factor for chemotherapy failure in head and neck cancer (38,39). Our study revealed that SOX9 is involved in drug excretion and cell invasion in R HSC-3 cells. These findings indicated that SOX9 may be a CSC marker of HNSCC.

In this study, we created a multidrug-resistant head and neck squamous cell carcinoma cell line and showed that multidrug-resistant cells exhibited characteristics of CSCs. Furthermore, analysis of the multidrug-resistant squamous cell carcinoma cells showed that not only CD44 and ABCG2 but also SOX9 may be new predictors of prognosis for head and neck cancer. We also showed that ABCG2, CD44, and SOX9 play roles in various CSC activities. However, this study was performed using *in vitro* experiments. Therefore, *in vivo* experiments will be required to evaluate whether these molecules affect tumor growth and drug resistance in mice.

Acknowledgements

Not applicable.

Funding

This investigation was supported in part by JSPS KAKENHI (grant nos. 17K11691, 17K11890 and 20K09947).

Availability of data and materials

The datasets used and/or analyzed during the current study are available from the corresponding author on reasonable request.

Authors' contributions

KM contributed to experimental design, performed the majority of experiments and drafted the manuscript. NU conducted experimental design of all experiments and data analysis and drafted the manuscript. MA performed some experiments and data analysis. MM participated in some experiments and data analysis. EO contributed to experimental conceptualization and drafted the manuscript. NU and EO confirm the authenticity of all the raw data. All authors read and approved the final manuscript.

Ethics approval and consent to participate

Not applicable.

Patient consent for publication

Not applicable.

Competing interests

The authors declare that they have no competing interests.

Authors' information

Dr Naoki Umemura, https://orcid.org/0000-0002-3249-782X;
Dr Makoto Adachi, https://orcid.org/0000-0002-9382-7052;
Dr Emika Ohkoshi, https://orcid.org/0000-0001-9700-9973.

References

1. Scadden DT: Cancer stem cells refined. Nat Immunol 5: 701-703, 2004.
2. Visvader JE and Lindeman GJ: Cancer stem cells: Current status and evolving complexities. Cell Stem Cell 10: 717-728, 2012.
3. Magee JA, Piskounova E and Morrison SJ: Cancer stem cells: Impact, heterogeneity, and uncertainty. Cancer Cell 21: 283-296, 2012.
4. Chen D, Wu M, Li Y, Chang L, Yuan Q, Ekimyan-Salvo M, Deng P, Yu B, Yu Y, Dong J, *et al*: Targeting BMI1+ cancer stem cells overcomes chemoresistance and inhibits metastases in squamous cell carcinoma. Cell Stem Cell 20: 621-634, 2017.
5. White RA, Neiman JM, Reddi A, Han G, Birlea S, Mitra D, Dionne L, Fernandez P, Murao K, Bian L, *et al*: Epithelial stem cell mutations that promote squamous cell carcinoma metastasis. J Clin Invest 123: 4390-4404, 2013.
6. Bao S, Wu Q, McLendon RE, Hao Y, Shi Q, Hjelmeland AB, Dewhirst MW, Bigner DD and Rich JN: Glioma stem cells promote radioresistance by preferential activation of the DNA damage response. Nature 444: 756-760, 2006.

7. Meacham CE and Morrison SJ: Tumour heterogeneity and cancer cell plasticity. Nature 501: 328-337, 2013.
8. Li J, Condello S, Thomes-Pepin J, Ma X, Xia Y, Hurley TD, Matei D and Cheng JX: Lipid desaturation is a metabolic marker and therapeutic target of ovarian cancer stem cells. Cell Stem Cell 20: 303-314 e305, 2017.
9. Codd AS, Kanaseki T, Torigo T and Tabi Z: Cancer stem cells as targets for immunotherapy. Immunology 153: 304-314, 2018.
10. Ohkoshi E and Umemura N: Induced overexpression of CD44 associated with resistance to apoptosis on DNA damage response in human head and neck squamous cell carcinoma cells. Int J Oncol 50: 387-395, 2017.
11. Nanbu T, Umemura N, Ohkoshi E, Nanbu K, Sakagami H and Shimada J: Combined SN-38 and gefitinib treatment promotes CD44 degradation in head and neck squamous cell carcinoma cells. Oncol Rep 39: 367-375, 2018.
12. Pena-Solorzano D, Stark SA, Konig B, Sierra CA and Ochoa-Puentes C: ABCG2/BCRP: Specific and nonspecific modulators. Med Res Rev 37: 987-1050, 2016.
13. Chen Z, Shi T, Zhang L, Zhu P, Deng M, Huang C, Hu T, Jiang L and Li J: Mammalian drug efflux transporters of the ATP binding cassette (ABC) family in multidrug resistance: A review of the past decade. Cancer Lett 370: 153-164, 2016.
14. Lu BC, Li J, Yu WF, Zhang GZ, Wang HM and Ma HM: Elevated expression of Nrf2 mediates multidrug resistance in CD133+ head and neck squamous cell carcinoma stem cells. Oncol Lett 12: 4333-4338, 2016.
15. Guan GF, Zhang DJ, Zheng Y, Wen LJ, Yu DJ, Lu YQ and Zhao Y: Significance of ATP-binding cassette transporter proteins in multidrug resistance of head and neck squamous cell carcinoma. Oncol Lett 10: 631-636, 2015.
16. Hu J, Li J, Yue X, Wang J, Liu J, Sun L and Kong D: Expression of the cancer stem cell markers ABCG2 and OCT-4 in right-sided colon cancer predicts recurrence and poor outcomes. Oncotarget 8: 28463-28470, 2017.
17. Xiong B, Ma L, Hu X, Zhang C and Cheng Y: Characterization of side population cells isolated from the colon cancer cell line SW480. Int J Oncol 45: 1175-1183, 2014.
18. Posner MR, Hershock DM, Blajman CR, Mickiewicz E, Winquist E, Gorbounova V, Tjulandin S, Shin DM, Cullen K, Ervin TJ, *et al*: Cisplatin and fluorouracil alone or with docetaxel in head and neck cancer. N Engl J Med 357: 1705-1715, 2007.
19. Bolstad BM, Irizarry RA, Astrand M and Speed TP: A comparison of normalization methods for high density oligonucleotide array data based on variance and bias. Bioinformatics 19: 185-193, 2003.
20. Gentleman RC, Carey VJ, Bates DM, Bolstad B, Dettling M, Dudoit S, Ellis B, Gautier L, Ge Y, Gentry J, *et al*: Bioconductor: Open software development for computational biology and bioinformatics. Genome Biol 5: R80, 2004.
21. Quackenbush J: Microarray data normalization and transformation. Nat Genet 32 Suppl: S496-S501, 2002.
22. Takeishi S and Nakayama KI: Role of Fbxw7 in the maintenance of normal stem cells and cancer-initiating cells. Br J Cancer 111: 1054-1059, 2014.
23. Takeishi S, Matsumoto A, Onoyama I, Naka K, Hirao A and Nakayama KI: Ablation of Fbxw7 eliminates leukemia-initiating cells by preventing quiescence. Cancer Cell 23: 347-361, 2013.
24. Saito Y, Uchida N, Tanaka S, Suzuki N, Tomizawa-Murasawa M, Sone A, Najima Y, Takagi S, Aoki Y, Wake A, *et al*: Induction of cell cycle entry eliminates human leukemia stem cells in a mouse model of AML. Nat Biotechnol 28: 275-280, 2010.
25. Kukal S, Guin D, Rawat C, Bora S, Mishra MK, Sharma P, Paul PR, Kanojia N, Grewal GK, Kukreti S, *et al*: Multidrug efflux transporter ABCG2: Expression and regulation. Cell Mol Life Sci 78: 6887-6939, 2021.
26. Fletcher JI, Haber M, Henderson MJ and Norris MD: ABC transporters in cancer: More than just drug efflux pumps. Nat Rev Cancer 10: 147-156, 2010.
27. Moniot B, Declosmenil F, Barrionuevo F, Scherer G, Aritake K, Malki S, Marzi L, Cohen-Solal A, Georg I, Klattig J, *et al*: The PGD2 pathway, independently of FGF9, amplifies SOX9 activity in Sertoli cells during male sexual differentiation. Development 136: 1813-1821, 2009.
28. Chaffer CL, Dopheide B, Savagner P, Thompson EW and Williams ED: Aberrant fibroblast growth factor receptor signaling in bladder and other cancers. Differentiation 75: 831-842, 2007.
29. Giancotti FG: Mechanisms governing metastatic dormancy and reactivation. Cell 155: 750-764, 2013.
30. Modok S, Mellor HR and Callaghan R: Modulation of multidrug resistance efflux pump activity to overcome chemoresistance in cancer. Curr Opin Pharmacol 6: 350-354, 2006.
31. Kage K, Tsukahara S, Sugiyama T, Asada S, Ishikawa E, Tsuruo T and Sugimoto Y: Dominant-negative inhibition of breast cancer resistance protein as drug efflux pump through the inhibition of S-S dependent homodimerization. Int J Cancer 97: 626-630, 2002.
32. Suresh R, Ali S, Ahmad A, Philip PA and Sarkar FH: The role of cancer stem cells in recurrent and drug-resistant lung cancer. Adv Exp Med Biol 890: 57-74, 2016.
33. Nieh S, Jao SW, Yang CY, Lin YS, Tseng YH, Liu CL, Lee TY, Liu TY, Chu YH and Chen SF: Regulation of tumor progression via the Snail-RKIP signaling pathway by nicotine exposure in head and neck squamous cell carcinoma. Head Neck 37: 1712-1721, 2015.
34. Wang J, Wu Y, Gao W, Li F, Bo Y, Zhu M, Fu R, Liu Q, Wen S and Wang B: Identification and characterization of CD133+CD44+ cancer stem cells from human laryngeal squamous cell carcinoma cell lines. J Cancer 8: 497-506, 2017.
35. Lee Y, Shin JH, Longmire M, Wang H, Kohrt HE, Chang HY and Sunwoo JB: CD44+ cells in head and neck squamous cell carcinoma suppress T-cell-mediated immunity by selective constitutive and inducible expression of PD-L1. Clin Cancer Res 22: 3571-3581, 2016.
36. Wagner T, Wirth J, Meyer J, Zabel B, Held M, Zimmer J, Pasantes J, Bricarelli FD, Keutel J, Hustert E, *et al*: Autosomal sex reversal and campomelic dysplasia are caused by mutations in and around the SRY-related gene SOX9. Cell 79: 1111-1120, 1994.
37. Tanaka J, Mabuchi Y, Hata K, Yasuhara R, Takamatsu K, Kujiraoka S, Yukimori A, Takakura I, Sumimoto H, Fukada T, *et al*: Sox9 regulates the luminal stem/progenitor cell properties of salivary glands. Exp Cell Res 382: 111449, 2019.
38. Khorani K, Schwaerzler J, Burkart S, Kurth I, Holzinger D, Flechtenmacher C, Plinkert PK, Zaoui K and Hess J: Establishment of a plasticity-associated risk model based on a SOX2- and SOX9-related gene set in head and neck squamous cell carcinoma. Mol Cancer Res 19: 1676-1687, 2021.
39. Al-Zahrani KN, Abou-Hamad J, Pascoal J, Labreche C, Garland B and Sabourin LA: AKT-mediated phosphorylation of Sox9 induces Sox10 transcription in a murine model of HER2-positive breast cancer. Breast Cancer Res 23: 55, 2021.